Journal of Aerosol Science 150 (2020) 105616

Contents lists available at ScienceDirect

Journal of Aerosol Science

journal homepage: http://www.elsevier.com/locate/jaerosci

Multiplexed electrospray emitters fabricated by rapid laser micromachining

Liurui Li [a,b], Weiwei Yang [a], Xinyan Zhao [a,c], Weiwei Deng [a,*]

[a] Department of Mechanics and Aerospace Engineering, Southern University of Science and Technology, Shenzhen, 518055, China
[b] Department of Mechanical Engineering, Virginia Polytechnic Institute and State University, Blacksburg, VA, 24061, USA
[c] Academy for Advanced Interdisciplinary Studies, Southern University of Science and Technology, Shenzhen, 518055, China

A B S T R A C T

This technical note documents the fabrication and performance of multiplexed electrospray emitters by rapid laser micromachining. A low cost 1064-nm fiber laser marker system is used to precisely, rapidly and selectively remove materials from a sheet of conductive silicone rubber, which is chemically inert. The laser pulse energy, scanning speed and machining path are judicially chosen to create clean and round micro posts that form external nozzle structures. This laser micromachining technique offers sufficient precision for ensuring uniform pressure drop across each fluid flow channel even at relatively low flow rate per nozzle. The uniformity of the operation from nozzle to nozzle is confirmed by measuring the diameter of each cone-jet. The results suggest that the laser micromachining is a rapid and convenient technique for fabricating multiplexed electrospray emitters.

1. Introduction

Electrospray (ES) is a versatile technique to generate aerosols with quasi-monodisperse droplets in the micrometer and even nanometer range (de la Mora et al., 1990; Gomez & Tang, 1994). In a typical electrospray setup, the polar or conducting liquid is fed to a capillary charged at high DC voltage, which establishes a strong electric field near the capillary. Under the combined action of electric stress and surface tension, the liquid at the capillary tip forms a Taylor cone (Taylor, 1964). A fine jet emanates from the cone apex and then breaks up into droplets via Rayleigh-Plateau instabilities. This phenomena, usually termed as the cone-jet mode electrospray (Cloupeau & Prunet-Foch, 1989; Ganan-Calvo, Lasheras, Dávila, & Barrero, 1994), has found numerous applications such as in analytical chemistry (Fenn, Mann, Meng, Wong, & Whitehouse, 1989), generation of biodegradable micro/nanoparticles (Almería, Deng, Fahmy, & Gomez, 2010), ultra-high resolution printing of advanced materials (Park, Jung, Park, Park, & Yoon, 2007), sensors (Matsushima, Yamazaki, Maeda, & Suzuki, 2004; Taylor & Velásquez-García, 2015), fabrication of piezoelectrics (García--Farrera & Velásquez-García, 2019; Rietveld, Kobayashi, Yamada, & Matsushige, 2006), and deposition of thin film photovoltaic devices (Jiang et al., 2018; Zhao et al., 2014). Because the diameter of droplets generated in the cone-jet mode is monotonically dependent on the flow rate, for applications that require smaller droplets, the flow-rate is correspondingly minuscule (A Gomez, Bingham, De Juan, & Tang, 1998). Therefore, multiplexed electrospray (MES) devices become indispensable for increasing the throughput of electrospray systems while preserving the small and uniform droplet size.

To date, at least five different fabrication methods for multiplexed electrospray have been reported: (i) independent assembly of individual capillaries (Dunn & Snarski, 1992; Rulison & Flagan, 1993; Regele, Papac, Rickard, & Dunn-Rankin, 2002; Hubacz & Marijnissen, 2003; Jaworek, Balachandran, Lackowski, Kulon, & Krupa, 2006; Si, Byun, & Lee, 2007; and; Marginean et al., 2008); (ii)

* Corresponding author.
E-mail address: dengww@sustech.edu.cn (W. Deng).

https://doi.org/10.1016/j.jaerosci.2020.105616
Received 11 May 2020; Received in revised form 8 June 2020; Accepted 15 June 2020
Available online 25 June 2020

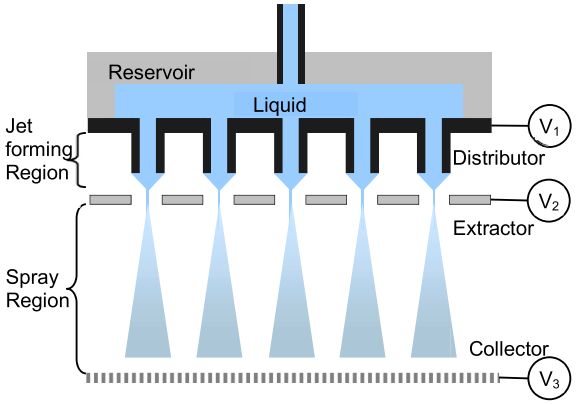

Fig. 1. The distributer-extractor-collector configuration of multiplexed electrospray.

silicon-based microfabrication (Xue et al., 1997; Xiong, Zhou, Sun, & Ye, 2005; Tai, Sniegoski, & Welch, 2002; Deng, Klemic, Li, Reed, & Gomez, 2006; Velasquez-Garcia, Akinwande, & Martinez-Sanchez, 2006; and W.; Kim, Guo, Yang, & Wang, 2007); (iii) soft lithography (J.-S. Kim & Knapp, 2001; Wang, Liu, Wang, Yao, & Yu, 2004; and Choi et al., 2011); (iv) additive manufacturing (Velásquez-García, 2015; Olvera-Trejo & Velásquez-García, 2016); and (v) conventional precision machining (Almekinders & Jones, 1999; Tang & Smith, 2001; Bocanegra, Galán, Márquez, Loscertales, & Barrero, 2005; Duby, Deng, Kim, Gomez, & Gomez, 2006; Tran et al., 2010; Lhernould & Lambert, 2011; and; Arnanthigo, Yurteri, Biskos, Marijnissen, & Schmidt-Ott, 2011). The subtractive manufacturing methods such as silicon-based microfabrication and conventional precision machining generally require many hours, if not days, of machining and assembly. For example, our group previously reported an approach of fabricating compact multiplexed electrospray emitter array from polycarbonate, brass, or aluminum using a precision CNC (Computer Numerical Control) machining platform (Lojewski, Yang, Duan, Xu, & Deng, 2013). The CNC machining, although reduces the turnaround time from weeks of silicon microfabrication to days, is still not rapid enough. This is because the moving speed of the machining tool must be kept as slow as ~1 mm/s to accommodate the constant acceleration and deceleration of coordinated x-y motions associated with circular or spiral paths for creating the small round nozzle structures. It takes the CNC about 30 min to mill a single nozzle, and an array of 100 nozzles will require two days of non-stop machining. Therefore, a rapid yet precision approach for machining multiple electrospray emitters is highly desirable.

Here we report the multiplexed electrospray emitters micromachined by a low cost laser marker that dramatically reduces the machining time for each nozzle by a factor of ~100 compared with CNC. Laser markers have become workhorses in the consumer electronics industry for engraving letters and logos on metal, glass and plastic surfaces of cell phone and tablets. The laser beam moving speed is amplified by scanning mirrors to as high as 5000 mm/s, which is three orders of magnitude faster than the motion of a physical micro milling bit. Combined with the focal point of ~10 μm, such laser marker is essentially a rapid and convenient micromachining tool with high precision. Indeed, we show that it only takes a few seconds to machine one nozzle, dramatically increasing the productivity of the micromachining process for multiplexed electrospray emitters.

2. Experimental

2.1. Overall design

The primary design goal of the MES device is to ensure each ES emitter operates in a similar way as the other. To that end, the design should meet two requirements: (i) the electric field near each cone-jet site is nearly identical and is not affected by other nozzles or the fluctuation of sprays; and (ii) the liquid flow rate passing through each nozzle is uniform.

To meet the first requirement, we adopted the three-electrode (emitter, extractor, and collector) configuration (Borra et al., 1999), which effectively separates the domain into two parts: the cone-jet forming region and the spray forming region (Fig. 1), so the space charge in the spray forming region does not affect the stable operation of the cone-jets, which are sensitive to the change in electric fields. The distance between the nozzle and the extractor is kept to be less than the inter-nozzle distance, therefore the electric field is primarily defined by the extractor instead of the neighboring nozzles. The electrode design should also address the “edge effect” (Deng et al., 2006), which refers to the fact that the nozzles at the edge of the array experience more intense electric filed and “pull” higher liquid flow rates from the edge nozzles, generating droplets that are significantly larger than those from inner nozzles. The strategy we used is to introduce extra dummy nozzles (posts without microfluidic channels) on the edge, which offset the edge effect and further improve the electric field uniformity.

To meet the second requirement, the flow impedance of the inner channel of the emitter should cause a pressure drop at least comparable with the electrohydrodynamic pulling pressure of the Taylor cone (Deng, Waits, Morgan, & Gomez, 2009). In other words, the viscous pressure drop modeled by the Poiseuille flow should be greater than the electrohydrodynamic pulling pressure, which is comparable to γ/OD. Here γ is the surface tension coefficient of the liquid, and OD is the nozzle outer diameter. Meanwhile, the fluidic

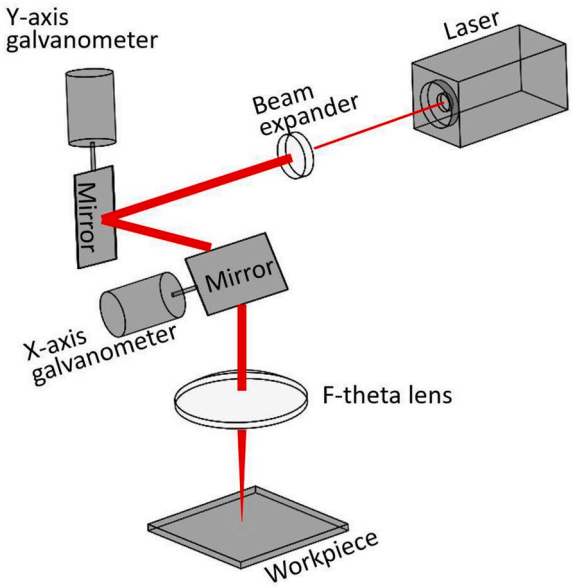

Fig. 2. Schematic of the working principle of laser marker.

design needs to be compatible with the geometry of the laser machining. Here we chose nozzle inner diameter ID = 55 μm, micro-channel length $L = 1500$ μm, nozzle height $H = 600$ μm, and outer diameter OD = 300 μm, We verified that those geometries meet the second requirement with ethanol running at ~1 ml/hr/nozzle. To ensure the electric field near each nozzle is similar, the nozzles should be well-separated, meaning the nozzle should be closer to the extractor than that to its neighboring nozzles. The distance between the nozzle and the extractor is at least 1.5 times of OD when both the height of Taylor cone and jet length are taken into account; hence the pitch L_p is chosen to be greater than 2 times of the OD. In this work, L_p is 0.75 mm (2.5 × OD) or 1 mm (3.33 × OD).

2.2. Device fabrication and assembly

We choose the 1.5 mm-thick electrically conductive grade silicone rubber sheet (CS Hyde Co., IL, USA) as the stock material for the ES emitter array for the following reasons. The conductive silicone is filled with ultra-fine carbon blacks and it offers several unique features that are suitable for electrospray emitters by laser machining. Silicone is odorless, tasteless and non-toxic. Especially, silicone is chemically inert to most solvents as well as acids which are often used as additives to enhance liquid conductivities. In fact, polydimethylsiloxane (PDMS) that has been widely used in microfluidics is one type of silicone. Silicone is hydrophobic, which is beneficial for forming Taylor cones. The embedded carbon blacks make the silicone sheet electrically conductive (with volume resistivity of 6 Ω/cm). Most importantly, the carbon black doped silicone sheet is non-transparent and can fully absorb the 1064 nm laser pulse energy for localized heating and vaporization, enabling effective and precise laser ablation even at modest laser power levels.

The principle of a laser marker is based on steering the pulsed and focused laser beam by two orthogonal scanning mirrors driven by galvanometers (Fig. 2). The pre-programmed machining pattern is realized by the two scanning mirrors combined with on/off control of the laser pulse. The laser marker used in this work is one of the most common and affordable models available under three thousand US dollars (RGL-FM-10 W, Rose Graphix). The key parameters of the laser are: wavelength 1064 nm, pulse width 200 ns, pulse frequency 20 kHz, scanning speed range 200–5000 mm/s, laser focal spot size 12 μm and the power range 2–10 W.

Initially the roundness of the laser drilled hole was rather disappointing (Fig. 3b and d). The reason is that as the laser beam hits the substrate, the rapid heating induces micro explosion and powder plumes that scatter subsequent laser pulses, significantly deteriorating the machining accuracy. After a few pulses a dimple is formed, which helps to confine the powder plumes and the machine quality is improved. Therefore the first a few pulses are most critical. To address this issue, we developed a machining recipe to improve the device finishing quality (Fig. 3a). We introduce a 120 μm thick conductive silicone layer on top of the 1.5 mm thick stock material to offset the non-circular portion. Fig. 3b shows the quality of the hole is significantly improved with the top layer. Similarly, the non-circular profile on the backside of the workpiece can be resolved by adding a bottom silicone layer. We call the top and bottom sheets as sacrifice layers. The sacrificial layers are the same type of silicone rubber as the MES emitters. We tested silicone sheets with different thickness, and found that when thickness is greater than 100 μm on the front, reasonably good circularity of the through hole can be achieved. We chose 120 μm to increase laser drilling depth. The thickness of the bottom sacrificial layer is not critical. The contact of the three layers is of the Van der Waals type as clean silicone surfaces tend to attach to each other. We first clean all contact surfaces with ethanol, then stack three layers together, and gently press the assembly to prevent large bubble from being trapped between layers. After machining, the sacrificial layers can be easily peeled off manually. Both the circularity and the uniformity of the

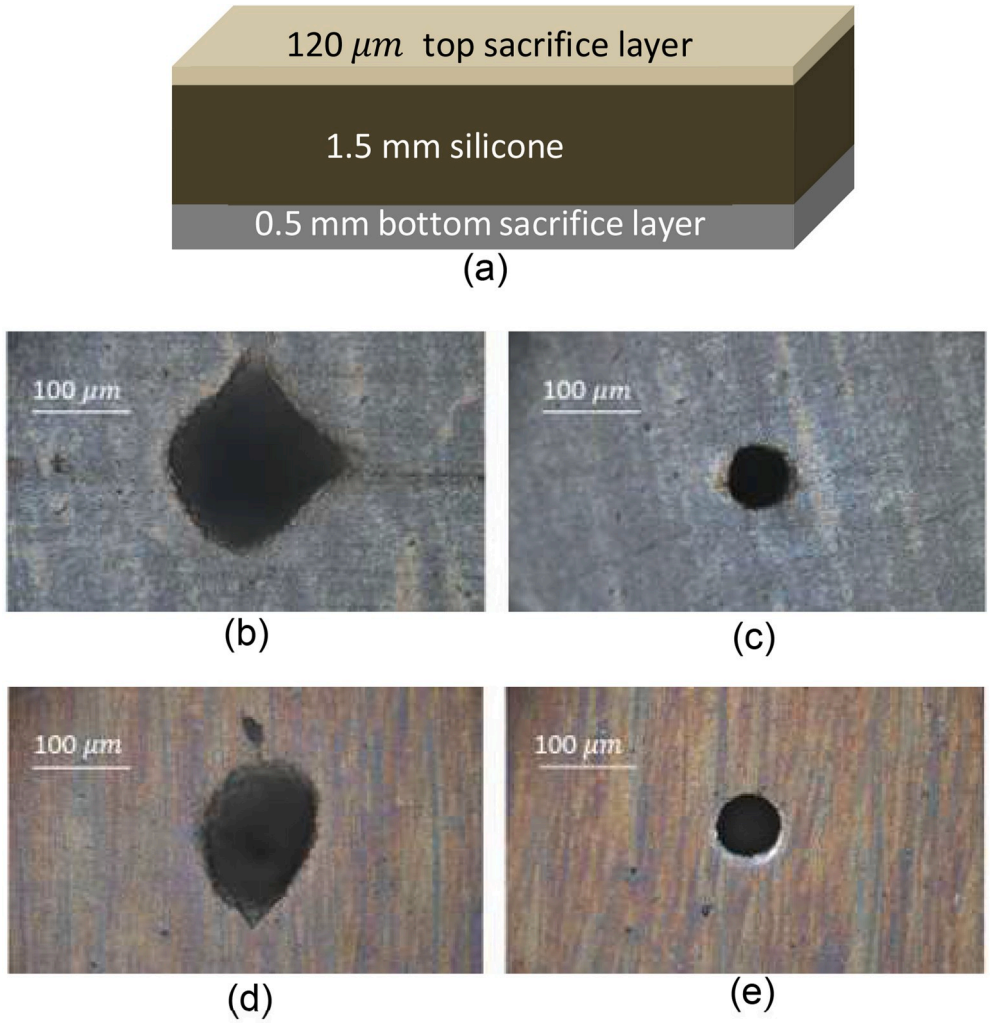

Fig. 3. (a) The 3-layer structure for improving machining quality. The final workpiece is sandwiched between the top and bottom sacrifice layers. (b) The frontside hole opening without top sacrifice layer. (c) The frontside hole opening with top sacrifice layer. (d) The backside hole opening without bottom sacrifice layer. (e) The backside hole opening with bottom sacrifice layer.

Table 1
Average inner diameter of through holes at different depth of the 1.5 mm silicone sheet.

Depth (μm)	0 (entry)	300	600	900	1200	1500(exit)
Average diameter (μm)	56.6	62.1	60.6	64.0	60.1	52.6
STDEV (μm)	2.3	2.3	2.3	2.3	2.4	2.4

through-hole array are significantly improved with the sacrifice layers.

We performed a metrology investigation of the microchannels (through holes) because the uniformity of the inner diameter is critical for distributing the flow evenly through each nozzle. We cut the 10-hole array into 5 thin slices and measured the hole diameter with the microscope. This gave us six sets of diameters for one through-hole array at different depths including entry and exit. Ten measurements were made for each data point. The data are summarized in Table 1. The results show that the relative standard deviation of the hole diameter is about 4%.

Fig. 4 shows the optical image (45° tilted view) of the nozzle array and the SEM image of a single nozzle machined by the laser marker. The nozzle outer diameter is 300 μm, inner diameter is 55 μm, and the height is 600 μm. The taper of the nozzle (Fig. 4b) is an artifact of the machining method. During laser machining, the material was removed layer by layer. The material removal of the present layer is accompanied with the "side burn" of the previously machined structure for the repeated laser paths. The tapered structure does not affect the overall operation of the MES emitters. The minimum outer diameter of the nozzle tested was 150 μm, but the wall of the 150 μm nozzles are too thin (~50 μm), and the ultrasonic cleaning sometime leads to the bending of those small nozzles.

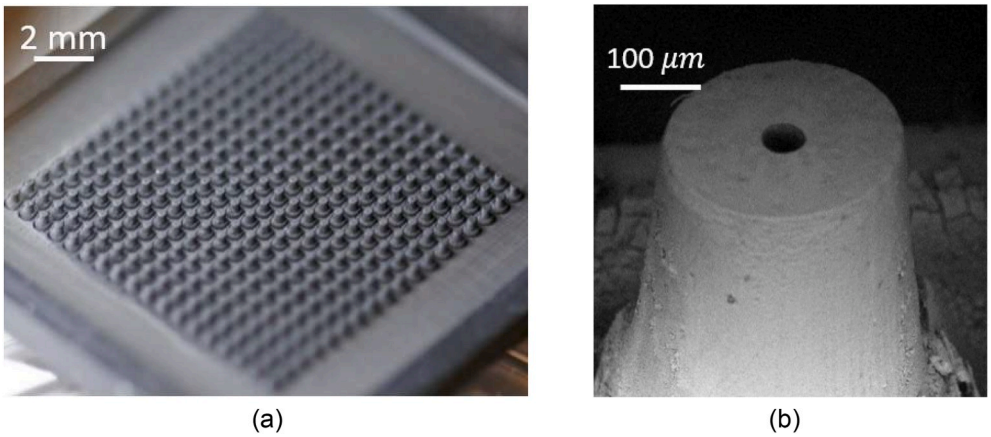

Fig. 4. (a) 16 × 16 nozzle array surrounded by dummy nozzles. (b) SEM image (45° tilted view) of a single nozzle.

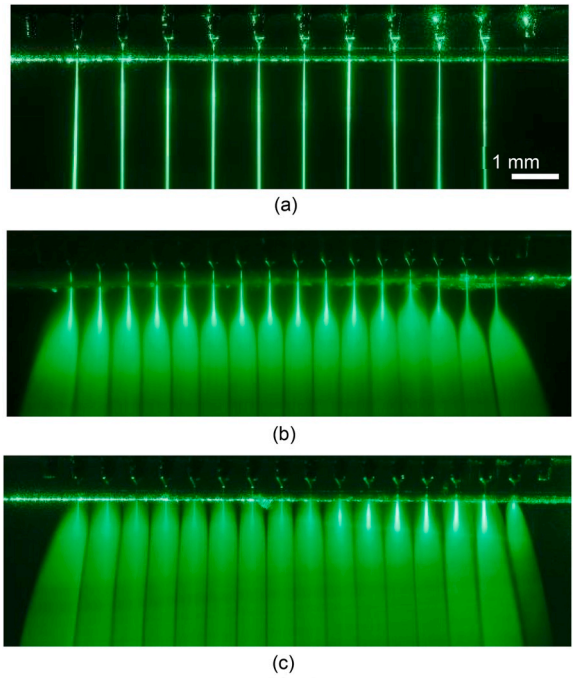

Fig. 5. The spray profile from the laser-machined linear emitter array at different liquid electrical conductivity k as well as average flow rate Q. (a) $k = 0.01$ μS/cm, $Q = 0.6$ mL/h/nozzle, number of nozzles: 10; (b) $k = 0.4$ μS/cm, $Q = 0.25$ mL/h/nozzle, number of nozzles: 16; and (c) $k = 4.2$ μS/cm, $Q = 0.25$ mL/h/nozzle, number of nozzles: 16. The driving field is the same (4.8 kV/cm) for all three cases.

Therefore we mostly worked with the 300 μm nozzles.

The extractor is an electrode positioned between the emitter and the collector to prevent the cone-jet from being influenced by the space charge created by sprays. The opening on the extractor can be through holes near each corresponding nozzle or simply a slot for a linear nozzle array. Either holes or the slot can allow droplets to pass through the cone-jet forming region and break up into fine droplets in the spray region. In this work, the hole array extractor was used for planar nozzle array while the slit design is used for a linear array. The slit extractor is a stainless steel foil of 100 μm in thickness with a 500 μm wide slit machined by the laser marker. The slit design is less prone to flooding while providing adequate electric field isolation.

The collector is the grounded electrode positioned below the extractor to provide sufficient driving electric field strength (a few kV/cm) to overcome the space charge. In order to prevent the liquid accumulation, the metal mesh is used as the collector.

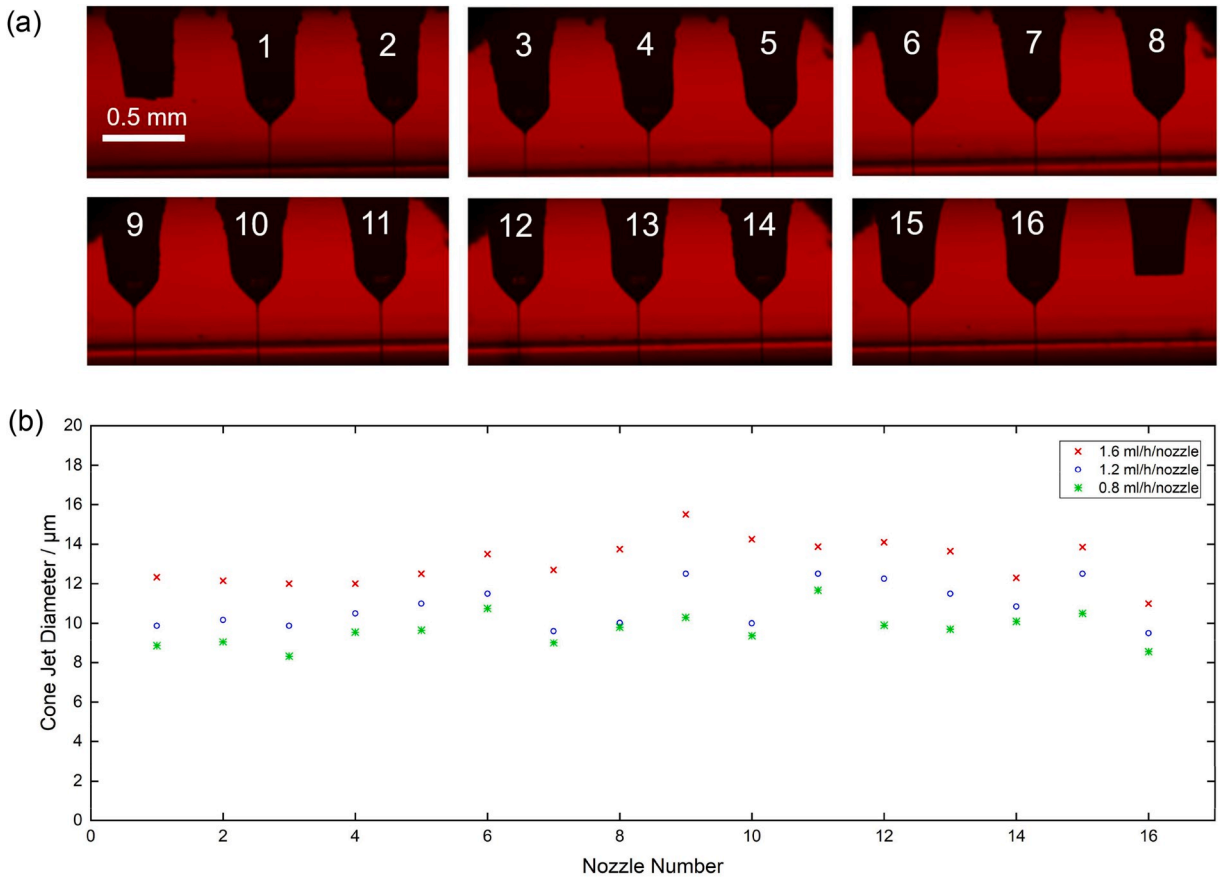

Fig. 6. The jet diameter uniformity from emitter to emitter. (a) The shadowgraph image taken by a DSLR coupled with long working distance microscope lens. Because the field of view is limited at high magnification, each image can only cover three nozzles. The left and right most posts are dummy nozzles. (b) The jet diameter measured from the images at different average flow rates of 0.8, 1.2 and 1.6 mL/h/nozzle. Emitter inner diameter: 55 μm, outer diameter 300 μm, pitch 0.75 mm.

3. Results and discussion

3.1. The critical driving field in the spray region

The driving field is an electric field maintained in the spray region between the extractor and the collector to continuously sweep the charged droplet to the collector. A prerequisite for stable operation of the MES system is that the driving field must be sufficiently strong to overcome the space charge field generated by sprays to prevent droplets from flying back to the extractor. In other words, the driving electric field must be greater than a critical value E_c, which is determined by the upper bound of the space charge field. For a linear multiplexed electrospray array, the space charge field is most intense near the center of the nozzle array, and the critical field can be estimated based on a line-of-charge model (Lojewski et al., 2013):

$$E_c \approx \ln(\frac{N}{2})\frac{\lambda}{\pi\varepsilon_0 L_0} \tag{1}$$

where N is the total number of emitters, ε_0 is the vacuum permittivity (8.854 pF/m), L_0 is the pitch between each nozzle, λ is the line charge density defined by $\lambda = I_0/v_z$. Here I_0 is the average current from a single emitter, and v_z is the droplet velocity. For the stable cone-jet of ethanol (200 proof) operated at the flow rate of 0.8 mL/h, I_0 is ~7 nA, v_z is ~10 m/s. For the 16-emitter linear array shown in Fig. 5, $L_0 = 0.75$ mm and $N = 16$, we find $E_c = 0.7$ kV/cm. Thus, the minimum driving field between the extractor and the collector is ~0.7 kV/cm in order to prevent droplets from flying back to the extractor. When spraying fluids with higher conductivity or higher flow rates, or both, the minimum driving field will be higher. For instance, when the conductivity of the liquid is increased to 1.4 μs/cm by doping the ethanol with NaCl water solution, the average current of each nozzle is increased from 7 nA to 13 nA, corresponding to the E_c of 1.3 kV/cm. In this study, the emitter and extractor are charged at 4.8 kV and 4.0 kV respectively. The collector is grounded.

Table 2
Diameter of cone-jets for the linear emitter array operated at different flow rates* (Fernandez de la Mora et al., 1990).

Flow rate (mL/h/nozzle)	0.8	1.2	1.6
Jet diameter (μm) estimated from 1st principles*	14.7	16.8	18.5
Measured average jet diameter (μm)	9.6	10.8	13.1
STDVE of jet diameter (μm)	0.86	1.10	1.14
RSD	8.9%	10.1%	8.7%

3.2. Multiplexed electrospray operation

To monitor the operation of the MES emitter, we first visualize the spray by shining a 532 nm laser sheet along the direction of the linear nozzle array.

Generally speaking, as the liquid conductivity increases, the droplet diameter decreases. Consequently, the droplet inertia becomes less important compared with the inter-droplet Coulombic repulsion force. Therefore, sprays of higher flow rates combined with lower conductivity exhibit narrow spray profiles, which sprays from liquids with high conductivities open up early to form spray plume. Fig. 5 clearly demonstrates the trend with liquids of different conductivities under the same driving field of 4.8 kV/cm. The liquid is supplied via a syringe pump (SyringeONE). For low conductivity $k = 0.01$ μS/cm and average flow rate of 0.6 mL/h/nozzle, the droplet diameter is relatively large and the inertia is significant, which causes the droplets remain a single file and form very narrow and well-separated sprays (Fig. 5a). With intermediate conductivity $k = 0.4$ μS/cm and average flow rate of 0.25 mL/h/nozzle, the sprays open up and merge with neighboring sprays ~2 mm away from the extractor (Fig. 5b). For relatively high conductivity $k = 4.2$ μS/cm and average flow rate: 0.25 mL/h/nozzle, the sprays appear to be very fine and open up immediately below the extractor (Fig. 5c).

The uniformity of the operation from emitter to emitter is verified by measuring the cone-jet diameter from optical micrographs. We use a red LED light source forming a shadowgraph configuration. A long working distance microscope object lens (Nikon Plan Fluor 10x with numerical aperture of 0.3) is coupled with the Canon 650D DSLR via an in-house built lens tube to acquire images with the resolution of 0.5 μm/pixel. The liquid conductivity is kept low to form thicker jets for higher accuracy of jet diameter measurements. Fig. 6 shows images of 16 nozzles with cone-jet mode together with two dummy nozzles at both ends of the nozzle array, from which we measured the diameter of jets. Three average flow rates tested are: 0.8, 1.2 and 1.6 mL/h/nozzle. The diameter of the cone jet would decrease slightly as the liquid jet pass the extractor, and we measure the jet diameter at the same vertical location (right above the extractor). For each jet, six images were taken to obtain the jet diameter. Fig. 6 shows the jet diameter distribution for all 16 emitters at different average flow rates. Table 2 summarizes the average diameter of cone jets and the relative standard deviation (RSD). The RSD is ~10%, suggesting a uniform operation across the emitter array.

4. Conclusion

In this Technical Note we document the design rationale, fabrication, and operation of silicone based, laser micro-machined multiplexed electrospray emitters. We used an inexpensive 1064-nm fiber laser marker to precisely and rapidly machine micro nozzle arrays out of a silicone sheet. The laser pulse energy and path are judiciously chosen to create clean and round micro posts that form the external structure of the nozzles. The use of sacrifice layers noticeably improve the machining quality of the nozzle, namely the roundness of the laser-drilled holes. The results suggest that the laser marker is fully capable of handling micro drilling, milling, and engraving tasks on the carbon black filled silicone sheets. The laser micromachining method strikes a good balance among precision, speed, convenience, and cost. Decent uniformity of the cone-jet diameter (RSD = 10%) among the entire multiplexed electrospray emitter array has been demonstrated.

Acknowledgement

We thank the National Natural Science Foundation of China (No. 11802115, 11932009, 61975073) for financial support.

References

Almekinders, J., & Jones, C. (1999). Multiple jet electrohydrodynamic spraying and applications. *Journal of Aerosol Science, 30*(7), 969–971.
Almería, B., Deng, W., Fahmy, T. M., & Gomez, A. (2010). Controlling the morphology of electrospray-generated PLGA microparticles for drug delivery. *Journal of Colloid and Interface Science, 343*(1), 125–133.
Arnanthigo, Y., Yurteri, C., Biskos, G., Marijnissen, J., & Schmidt-Ott, A. (2011). Out-scaling electrohydrodynamic atomization systems for the production of well-defined droplets. *Powder Technology, 214*(3), 382–387.
Bocanegra, R., Galán, D., Márquez, M., Loscertales, I., & Barrero, A. (2005). Multiple electrosprays emitted from an array of holes. *Journal of Aerosol Science, 36*(12), 1387–1399.
Borra, J., Camelot, D., Chou, K.-L., Kooyman, P., Marijnissen, J., & Scarlett, B. (1999). Bipolar coagulation for powder production: Micro-mixing inside droplets. *Journal of Aerosol Science, 30*(7), 945–958.
Choi, K.-H., Muhammad, N. M., Dang, H.-W., Lee, A., Hwang, J.-S., Nam, J. W., et al. (2011). Electrospray deposition of thin copper-indium-diselenide films. *International Journal of Materials Research, 102*(10), 1252–1260.
Cloupeau, M., & Prunet-Foch, B. (1989). Electrostatic spraying of liquids in cone-jet mode. *Journal of Electrostatics, 22*(2), 135–159.
Deng, W., Klemic, J. F., Li, X., Reed, M. A., & Gomez, A. (2006). Increase of electrospray throughput using multiplexed microfabricated sources for the scalable generation of monodisperse droplets. *Journal of Aerosol Science, 37*(6), 696–714.
Deng, W., Waits, C. M., Morgan, B., & Gomez, A. (2009). Compact multiplexing of monodisperse electrosprays. *Journal of Aerosol Science, 40*(10), 907–918.

Duby, M.-H., Deng, W., Kim, K., Gomez, T., & Gomez, A. (2006). Stabilization of monodisperse electrosprays in the multi-jet mode via electric field enhancement. *Journal of Aerosol Science, 37*(3), 306–322.
Dunn, P. F., & Snarski, S. R. (1992). Droplet diameter, flux, and total current measurements in an electrohydrodynamic spray. *Journal of Applied Physics, 71*(1), 80–84.
Fenn, J. B., Mann, M., Meng, C. K., Wong, S. F., & Whitehouse, C. M. (1989). Electrospray ionization for mass spectrometry of large biomolecules. *Science, 246*(4926), 64–71.
Ganan-Calvo, A., Lasheras, J., Dávila, J., & Barrero, A. (1994). The electrostatic spray emitted from an electrified conical meniscus. *Journal of Aerosol Science, 25*(6), 1121–1142.
García-Farrera, B., & Velásquez-García, L. F. (2019). Ultrathin ceramic piezoelectric films via room-temperature electrospray deposition of ZnO nanoparticles for printed GHz devices. *ACS applied materials & interfaces, 11*(32), 29167–29176.
Gomez, A., Bingham, D., De Juan, L., & Tang, K. (1998). Production of protein nanoparticles by electrospray drying. *Journal of Aerosol Science, 29*(5-6), 561–574.
Gomez, A., & Tang, K. (1994). Charge and fission of droplets in electrostatic sprays. *Physics of Fluids, 6*(1), 404–414.
Hubacz, A., & Marijnissen, J. (2003). The scale-up of electrohydrodynamic atomization. *Journal of Aerosol Science, 34*(Suppl. 1), S1269–S1270.
Jaworek, A., Balachandran, W., Lackowski, M., Kulon, J., & Krupa, A. (2006). Multi-nozzle electrospray system for gas cleaning processes. *Journal of Electrostatics, 64*(3-4), 194–202.
Jiang, Y., Wu, C., Li, L., Wang, K., Tao, Z., Gao, F., et al. (2018). All electrospray printed perovskite solar cells. *Nanomaterials and Energy, 53*, 440–448.
Kim, W., Guo, M., Yang, P., & Wang, D. (2007). Microfabricated monolithic multinozzle emitters for nanoelectrospray mass spectrometry. *Analytical Chemistry, 79*(10), 3703–3707.
Kim, J.-S., & Knapp, D. R. (2001). Microfabrication of polydimethylsiloxane electrospray ionization emitters. *Journal of Chromatography A, 924*(1-2), 137–145.
Lhernould, M. S., & Lambert, P. (2011). Compact polymer multi-nozzles electrospray device with integrated microfluidic feeding system. *Journal of Electrostatics, 69*(4), 313–319.
Lojewski, B., Yang, W., Duan, H., Xu, C., & Deng, W. (2013). Design, fabrication, and characterization of linear multiplexed electrospray atomizers micro-machined from metal and polymers. *Aerosol Science and Technology, 47*(2), 146–152.
Marginean, I., Kelly, R. T., Prior, D. C., LaMarche, B. L., Tang, K., & Smith, R. D. (2008). Analytical characterization of the electrospray ion source in the nanoflow regime. *Analytical Chemistry, 80*(17), 6573–6579.
Matsushima, Y., Yamazaki, T., Maeda, K., & Suzuki, T. (2004). Fabrication of SnO 2 particle-layers using the electrospray method and gas sensing properties for H 2. *Journal of Electroceramics, 13*(1-3), 765–770.
Fdela Mora, J., Navascues, J., Fernandez, F., & Rosell-Llompart, J. (1990). Generation of submicron monodisperse aerosols in electrosprays. *Journal of Aerosol Science, 21*(SUPPL. 1), S673–S676.
Olvera-Trejo, D., & Velásquez-García, L. (2016). Additively manufactured MEMS multiplexed coaxial electrospray sources for high-throughput, uniform generation of core–shell microparticles. *Lab on a Chip, 16*(21), 4121–4132.
Park, J. W., Jung, W. S., Park, S. R., Park, B. C., & Yoon, Y. J. (2007). Analysis of intracellular short organic acid-coenzyme A esters from actinomycetes using liquid chromatography-electrospray ionization-mass spectrometry. *Journal of Mass Spectrometry, 42*(9), 1136–1147.
Regele, J., Papac, M., Rickard, M., & Dunn-Rankin, D. (2002). Effects of capillary spacing on EHD spraying from an array of cone jets. *Journal of Aerosol Science, 33*(11), 1471–1479.
Rietveld, I. B., Kobayashi, K., Yamada, H., & Matsushige, K. (2006). Morphology control of poly(vinylidene fluoride) thin film made with electrospray. *Journal of Colloid and Interface Science, 298*(2), 639–651.
Rulison, A. J., & Flagan, R. C. (1993). Scale-up of electrospray atomization using linear arrays of Taylor cones. *Review of Scientific Instruments, 64*(3), 683–686.
Si, B. Q. T., Byun, D., & Lee, S. (2007). Experimental and theoretical study of a cone-jet for an electrospray microthruster considering the interference effect in an array of nozzles. *Journal of Aerosol Science, 38*(9), 924–934.
Tai, S. S., Sniegoski, L. T., & Welch, M. J. (2002). Candidate reference method for total thyroxine in human serum: Use of isotope-dilution liquid chromatography-mass spectrometry with electrospray ionization. *Clinical Chemistry, 48*(4), 637–642.
Tang, K., & Smith, R. D. (2001). Physical/chemical separations in the break-up of highly charged droplets from electrosprays. *Journal of the American Society for Mass Spectrometry, 12*(3), 343–347.
Taylor, G. I. (1964). Disintegration of water drops in an electric field. Proceedings of the Royal Society of London. Series A. *Mathematical and Physical Sciences, 280*(1382), 383–397.
Taylor, A. P., & Velásquez-García, L. F. (2015). Electrospray-printed nanostructured graphene oxide gas sensors. *Nanotechnology, 26*(50), 8, 505301.
Tran, S. B. Q., Byun, D., Nguyen, V. D., Yudistira, H. T., Yu, M. J., Lee, K. H., et al. (2010). Polymer-based electrospray device with multiple nozzles to minimize end effect phenomenon. *Journal of Electrostatics, 68*(2), 138–144.
Velásquez-García, L. F. (2015). SLA 3-D printed arrays of miniaturized, internally fed, polymer electrospray emitters. *Journal of Microelectromechanical Systems, 24*(6), 2117–2127.
Velasquez-Garcia, L. F., Akinwande, A. I., & Martinez-Sanchez, M. (2006). A micro-fabricated linear array of electrospray emitters for thruster applications. *Journal of Microelectromechanical Systems, 15*(5), 1260–1271.
Wang, J., Liu, J., Wang, X., Yao, J., & Yu, Z. (2004). Application of electrospray ionization mass spectrometry in rapid typing of fengycin homologues produced by Bacillus subtilis. *Letters in Applied Microbiology, 39*(1), 98–102.
Xiong, J., Zhou, Z., Sun, D., & Ye, X. (2005). Development of a MEMS based colloid thruster with sandwich structure. Sensors and actuators A. *Physica, 117*(1), 168–172.
Xue, Q., Foret, F., Dunayevskiy, Y. M., Zavracky, P. M., McGruer, N. E., & Karger, B. L. (1997). Multichannel microchip electrospray mass spectrometry. *Analytical Chemistry, 69*(3), 426–430.
Zhao, X.-Y., Wang, X., Lim, S. L., Qi, D., Wang, R., Gao, Z., et al. (2014). Enhancement of the performance of organic solar cells by electrospray deposition with optimal solvent system. *Solar energy materials and solar cells, 121*, 119–125.